Graft incompatibility between pepper and tomato can be attributed to genetic incompatibility between diverged immune systems

Thomas, Hannah Rae[1,2], Gevorgyan, Alice[1,4], Hermanson, Alexandra[1]., Yanders, Samantha[1], Erndwein, Lindsay[3,5], Norman-Ariztía, Matthew[1], Sparks Erin E.[3], Frank, Margaret H[1].

1. Cornell University, School of Integrative Plant Science, Ithaca, NY 14850, USA
2. John Innes Centre, Department of Cell and Developmental Biology, Norwich UK
3. University of Delaware, Department of Plant and Soil Sciences, Newark, DE 19713, USA
4. Stanford University, Department of Biology, Stanford, CA 94305, USA
5. USDA-ARS, Genetic Improvement for Fruits and Vegetables Laboratory, Chatsworth, NJ 08019, USA

Co- Corresponding authors: Hannah Rae Thomas (Hannah.Thomas@jic.ac.uk), Margaret H. Frank (mhf47@cornell.edu)

Date of submission: March 29, 2024

Total word count (less than 6500)	6198	No. of figures	8
Summary	200	No. of Tables	0
Introduction	843	No of Supporting files	14 Figures 20 Tables 13 Methods
Materials and Methods	501		
Results	3535		
Discussion	1022		
Acknowledgments	97		

Summary

- Graft compatibility is the capacity of two plants to form cohesive vascular connections. Tomato and pepper are incompatible graft partners; however, the underlying cause of graft rejection between these two species remains unknown.
- We diagnosed graft incompatibility between tomato and diverse pepper varieties based on weakened biophysical stability, decreased growth, and persistent cell death using trypan blue and TUNEL assays. Transcriptomic analysis of cell death in the junction was performed using RNA-sequencing, and molecular signatures for incompatible graft response were characterized based on meta-transcriptomic comparisons with other biotic processes.
- We show that tomato is broadly incompatible with diverse pepper cultivars. These incompatible graft partners activate prolonged transcriptional changes that are highly enriched for defense processes. Amongst these processes was broad NLR upregulation and hypersensitive response. Using transcriptomic datasets for a variety of biotic stress treatments, we identified a significant overlap in the genetic profile of incompatible grafting and plant parasitism. In addition, we found over 1000 genes that are uniquely upregulated in incompatible grafts.
- Based on NLR overactivity, DNA damage, and prolonged cell death we have determined that tomato and pepper graft incompatibility is likely caused by a form of genetic incompatibility, which triggers a hyperimmune-response.

Keywords:

autoimmunity, graft compatibility, hypersensitive response, programmed cell death, plant grafting, Solanaceae

Introduction

Grafting is an ancient agricultural practice that is used to propagate plants and combine desirable traits between independent root and shoot systems (Harrison & Burgess, 1962; Mudge *et al.*, 2009; Warschefsky *et al.*, 2016; Williams *et al.*, 2021). The apical portion of a graft is known as the scion and the root system is known as the rootstock (Scion:Rootstock). The capacity for two individuals to form continuous vascular connections across the graft site is known as graft compatibility (Harrison & Burgess, 1962; Moore, 1984). The inability to graft is categorized into two types of incompatibility: immediate incompatibility and delayed incompatibility (Mendel, 1936; Argles, 1937). Delayed incompatibility can present months or years after grafting, with symptoms such as swollen, over-proliferated scions, cell death in the junction, and structural instability of the stem (Eames & Cox, 1945; Moore & Walker, 1981; Andrews & Marquez, 2010). Despite a long history of grafting, humans still struggle to understand the mechanisms underlying graft incompatibility. Currently, there are only a few examples where the causes of incompatibility have been identified (Gur, 1968; Mosse & Herrero, 1951; Moore, 1986). Although there is likely a variety of species-specific cellular mechanisms that determine compatible versus incompatible graft pairings, the presence of persistent cell death in the junction is a common symptom that is observed across diverse plant families (Eames & Cox, 1945; Moore & Walker, 1981).

Cell death can be classified into two main categories: necrosis and programmed cell death (PCD; Burbridge *et al.*, 2007). Necrosis is defined as uncontrolled death and is often caused by stressors such as extreme heat, radiation, or a loss of membrane potential that is so intense that genetic processes are unable to act (Hirsch *et al.*, 1997; Burbridge *et al.*, 2007). In contrast, PCD is the controlled and organized process of cellular destruction (Lockshin & Zakeri, 2004).

All eukaryotes have evolved an innate immune system that is capable of detecting conserved foreign molecules during infection (Janeway et al., 2001). In plants, various elicitors such as pathogen associated molecular patterns (PAMPs) and damage associated molecular patterns (DAMPs) are perceived by membrane bound pattern recognition receptors (PRRs) facing the apoplast (Jones & Dangl, 2006; Amarante-

Mendes *et al.*, 2018; Steinbrenner *et al.*, 2020). These molecules trigger downstream pattern triggered immunity (PTI) and signal basal defense processes such as reactive oxygen species (ROS) production (Boller & He, 2009). Alternatively, some pathogens release effector proteins, which are expressed into the symplast to modify host responses and promote infection (Stergiopoulos & de Wit, 2009). These effectors are locked in an arms race with intracellular nucleotide-binding and leucine-rich repeat receptors (NLRs), which perceive effectors or proteins modified by effectors and elicit effector triggered immunity (ETI) and PCD (Wu *et al.*, 2014). Currently, no such molecules, apoplastic or symplastic, have been identified as the underlying cause of graft incompatibility, where an unknown signal from one graft partner is perceived by a protein of the other, thus leading to incompatibility.

Our previous work identified tomato and pepper as an herbaceous model for delayed incompatibility (Thomas *et al.*, 2022, 2023). Despite several studies investigating pepper graft compatibility, much remains unknown about the underlying mechanism (Deloire & Hébant, 1982; Ives, 2012; Kawaguchi *et al.*, 2008; Zeist *et al.*, 2018). To explore this, we grafted tomato to *Capsicum annuum* varieties, Cayenne, Doux des Landes, California Wonder, and *Capsicum chinense* variety Habanero. We found that tomato-*Capsicum* heterografts are all incompatible and exhibit failed xylem reconnections, weakened stem stability, and reduced growth. Using the tomato-pepper combination with the highest graft survival rate, tomato to California Wonder, we analyzed the presence of non-viable tissue in the junction at 7, 14, and 21 days after grafting (DAG), and investigated the cause using viability staining and transcriptomics. In contrast to self-grafted controls that clear non-viable tissue from the junction, we found that incompatible grafts exhibit persistent cell death at the junction. Additionally, we utilized RNA-seq to show that incompatible grafts have a prolonged defense response following grafting, including significant upregulation of many NLRs and signaling components involved in hypersensitive response (HR). Furthermore, we identified a set of potential incompatibility marker genes that are upregulated in incompatible junctions of both tomato and pepper stems. To characterize the molecular response of incompatible grafting in relation to other biotic stress responses, we conducted a transcriptomic meta-analysis comparing the effect of grafting with pathogen infection, herbivory, and plant parasitism. We found a significant overlap

in expression patterns between grafting and plant parasitism, indicating similar mechanisms underpin interspecies plant-to-plant interactions. Lastly, we identified a suite of over 1000 genes that are uniquely upregulated in incompatible grafts but not other biological stressors; among these genes, we identified genetic processes involved in immune responses and DNA damage. Together, this work supports a model in which tomato and pepper exhibit genetic incompatibility, which is potentially induced by incompatible cross-species NLRs that trigger the production of defensive compounds, upregulate programmed cell death, and eventually lead to genotoxic DNA damage. Genetic incompatibility between tomato and pepper would be the first identified instance of a hyper-immunity based incompatibility in a cross-species grafted crop.

Materials and methods

Plant materials and growth conditions

Capsicum annuum var. California Wonder (CW), RC Cayenne (Cayenne),Doux des Landes (DDL), and *Capsicum chinense* var. Habanero and *Capsicum chinense* (pepper), and *Solanum lycopersicum* (tomato) seeds were used for graft compatibility screening (Method S1). 21 day old pepper seedlings and 14 day old tomato seedlings were grafted (Method S2-3).

Characterizing graft compatibility

30 DAG the vascular connectivity of tomato and pepper junctions was assayed using propidium iodide staining (Method S4). Graft junction integrity was tested using manual bending (Thomas *et al.*, 2022). (Method S5). *Capsicum annuum* var. CW and *Solanum lycopersicum* Var. M82 were used to conduct 3-point bend tests at the University of Delaware. Structural mechanics of the graft junction were assessed by 3-point bend testing (Method S6) (Ennos *et al.*, 1993; Goodman & Ennos, 2001; Hostetler *et al.*, 2022).

DAMP Assay

Hypocotyl explants from *Capsicum annuum* var. CW and *Solanum lycopersicum* Var. M82 were placed on callus-inducing media for 7 days (Method S7). The hypocotyl tissue was then placed onto media which either previously cultured tomato or pepper tissue for

7 additional days. The area of the explants was measured after 7 days on the experimental media.

Grafting for TUNEL, trypan blue staining, and RNA-seq

Capsicum annuum var. (CW) and *Solanum lycopersicum* Var. M82 were grown as described above. 36 of each tomato and pepper species were left ungrafted. The rest of the plants were grafted as described above in the following combinations: 50 tomato:tomato, 50 CW:CW, 70 tomato:CW, and 70 CW:tomato. Ungrafted CW and tomato plants were included in the recovery procedure. Plastic domes were vented 7 DAG and removed 14 DAG.

Trypan Blue staining

Stems from 7, 14, 21 DAG, and ungrafted plants were collected and stained with 1% Trypan Blue as previously reported (Method S8; Fernández-Bautista, 2016).

TUNEL Assay

A 0.5 cm piece of the junction from 7, 14, 21 DAG, and ungrafted plants were used to image PCD. Assays were performed using the Promega DeadEnd™ Fluorometric TUNEL System (Method S9).

Transcriptomic Analysis

Capsicum annuum var. CW and *Solanum lycopersicum* Var. M82 were grafted as previously described. A 0.5 cm of the junctions of 7, 14, 21 DAG, and ungrafted plants were collected from 5 biological replicates for each sample. Each piece of tissue was flash-frozen and ground with a mortar and pestle. Total RNA was purified and 3' Seq libraries were constructed at the Cornell Institute of Biotechnology, Biotechnology Resource Center, and the libraries were sequenced on an Illumina NextSeq 500/550 using an Illumina High-output kit (Method S10). Fasta files were processed to yield raw reads and differential expression analysis was performed using DESeq2 (Method S10; Love *et al.*, 2014). Putative orthogroups were determined using OrthoFinder with Diamond as the sequence search program (Method S11; Buchfink *et al.*, 2014; Emms &

Kelly, 2019). Publicly available RNA-seq data was downloaded and processed to yield raw read counts (Method S12).

Statistical analysis and image analysis

All statistical computation and graph generation were performed in R v4.1.2 (R Core Team, 2021) (Method S13).

Results

Incompatible tomato and pepper heterografts are characterized by low survival, reduced growth, failed vascular connectivity, and physical instability

To investigate grafting between *Solanum lycopersicum* (tomato) and *Capsicum* (pepper) species, we performed a graft compatibility assay between self- and reciprocal grafts of *Solanum lycopersicum* var. M82 and *Capsicum annuum* varieties Cayenne, Doux des Landes (DDL), California Wonder (CW), and *Capsicum chinense* var. Habanero 30 DAG (Fig. 1, Fig. S1a-d, Table S1). Compared with self-grafted controls, heterografted tomato/pepper combinations exhibited significantly lower survival and higher break rates based on bend testing (Fig. 1a). Despite a low survival rate, self-grafted DDL plants that persisted formed strong graft junctions and were able to withstand the bend test (Moore, 1983; Thomas *et al.*, 2022, 2023). Previous work reported DDL as a compatible graft partner with tomato, yet when we challenged the integrity of the graft using the bend test, the plants broke at the junction 92% of the time, indicating a high level of incompatibility that was previously undetected (Deloire & Hébant, 1982). We also analyzed growth of the grafted shoot and root systems to test for developmental restrictions. Compatible shoot and root systems were 92.7% and 38.2% larger than incompatible plants (Figure 1b-c, Table S2). Additionally, the scion and stock diameters 2 cm above or below the junction were significantly restricted in their lateral development in incompatible grafts compared to self-grafted controls (Kruskal-Wallis Fig. S2a-b).

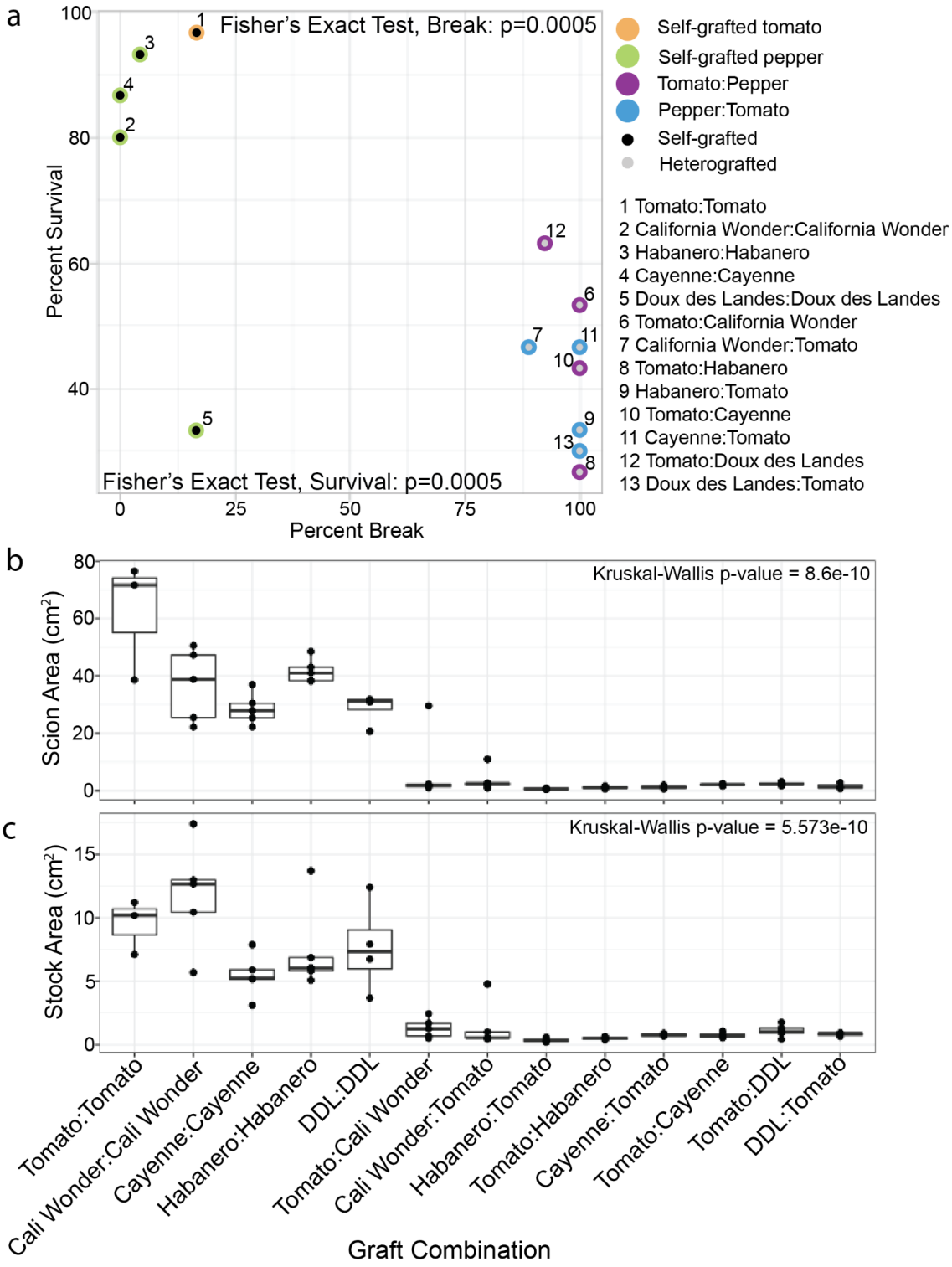

Figure 1: Heterografted tomato and pepper combinations exhibit moderate survival, unstable stem integrity, and reduced growth.
(a) The relationship between percent survival (y-axis) and percent break (x-axis) is shown for all graft combinations. Black dots denote self-grafts, grey dots denote heterografts. Self-grafted tomato is outlined in orange. Self-grafted pepper is outlined in

green. Heterografts where the scion is tomato are outlined in purple. Heterografts where the stock is tomato are outlined in blue. The identity of each data point is labeled 1-13. Percent survival n=30; For bend test sample size see Table S1. (b) The change in stem diameter 2cm above the graft junction between 30 and 0 DAG (scion). (c) The change in stem diameter 2 cm below the graft junction between 30 and 0 DAG (stock). California Wonder abbreviated to Cali Wonder, Doux des Landes abbreviated to DDL. Biological replicates are depicted as jitter and described in Table S2. Kruskal–Wallis one-way analysis of variance was used to detect significant differences between self- and heterografted combinations. p-value <0.05.

To examine the vascular connectivity of the grafts, we analyzed the anatomical organization of junctions from every tomato/pepper combination 30 DAG (Fig. 2). Consistent with our previous findings (Thomas *et al.*, 2023), all self-grafted combinations formed continuous xylem bridges across the graft junction (Fig. 2b, d, j, p, v), demonstrating compatibility (Moore, 1981; Melnyk *et al.*, 2015; Thomas *et al.*, 2022). Tomato grafted to any of the pepper varieties, formed non-vascular parenchymatous connections across the graft but failed to form xylem bridges (Fig. 2f, h, l, n, r, t, x, z). We noticed that overproliferated callus (Fig. 2l,t,x), as well as adventitious root growth (Fig. 2f, n, t) were common features in these incompatible combinations.

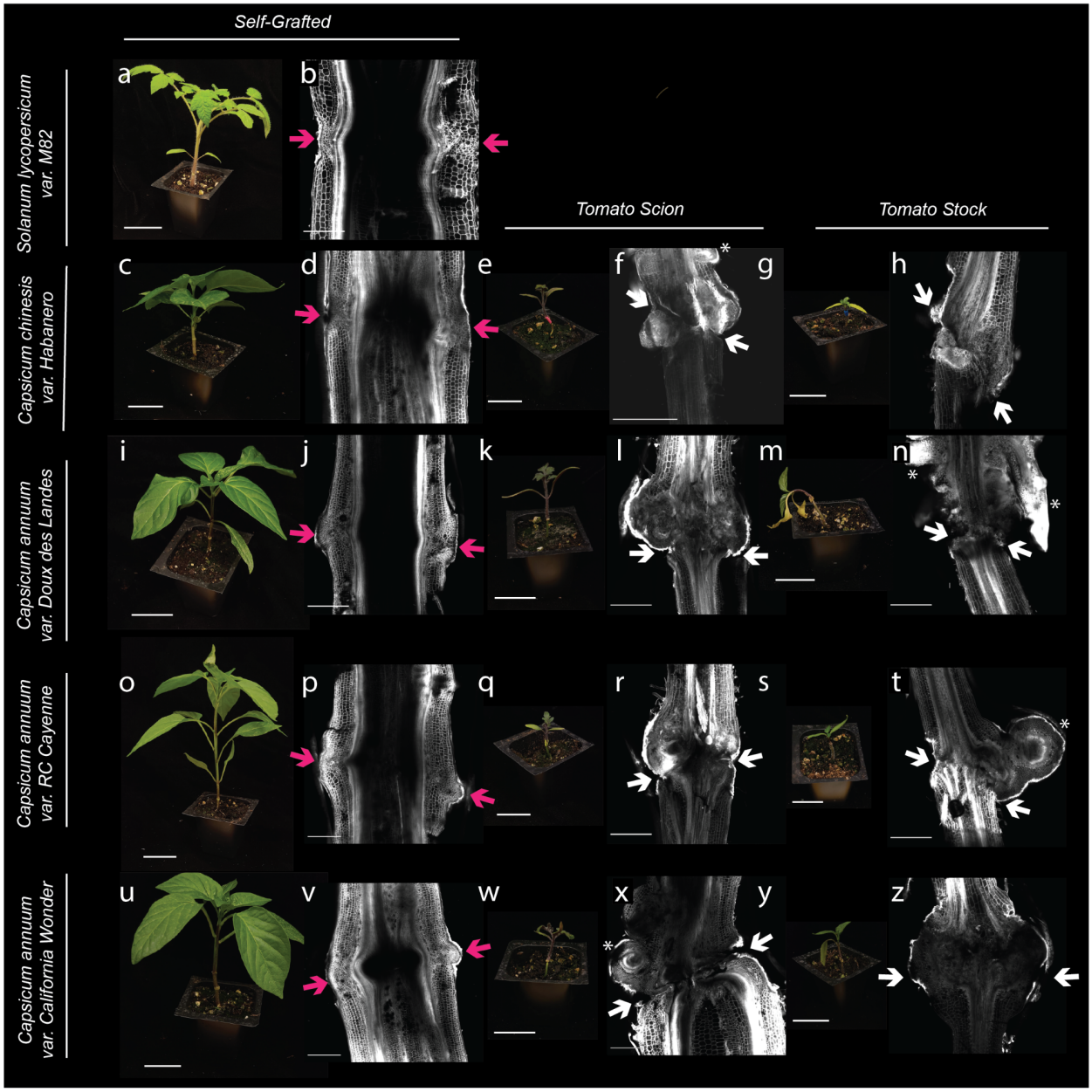

Figure 2: Heterografted pepper fails to form vascular connections and shows a significant decrease in size 30 DAG. (a, c, e, g, i, k, m, o, q, s, w, u, w, y) Representative photographs and (b, d, f, h, j, l, n, p, r, t, v, x, z) confocal micrographs for self-grafted tomato (a-b), self-grafted habanero (c-d), tomato:Habanero (e-f), Habanero:tomato (g-h), self-grafted Doux des Landes (DDL) (i-j), tomato:DDL (k-l), DDL:tomato (m-n). self-grafted Cayenne (o-p), tomato:Cayenne (q-r), Cayenne:tomato (s-t), self-grafted California Wonder (CW) (u-v), tomato:CW (w-x), CW:tomato (y-z). Graft junctions were stained with propidium iodide and imaged on a confocal microscope. Pink arrows indicate a successful graft junction with a healed xylem, white arrows indicate a failed vascular reconnection and white Asterix highlight adventitious

roots. All plant images have scale bars are 5 cm, and all micrograph scale bars are 1000 µm.

Because CW exhibited high survival rates when heterografted with tomato, we selected this genotype for further analysis. Incompatible grafts are commonly discovered when the junction breaks, due to failed vascular connectivity or cell death in the junction (Eames & Cox, 1945; Moore & Walker, 1981; Andrews & Marquez, 2010). With a better understanding of the vascular anatomy of compatible and incompatible plants, we sought to determine if we could quantify the instability observed in the manual bend test using a quantitative 3-point bend test. Congruent with reduced biophysical stability observed with the 3-point bend test, we found that there was a significant reduction in the structural stiffness of the heterografted junctions compared to self- and ungrafted stems (Fig. S1e-f, Table S3).

Incompatible graft junctions accumulate significantly more non-viable tissue than compatible grafts

Cell death is a common symptom associated with incompatible grafts (Moore, 1983). To examine the extent to which tomato/pepper (CW variety) heterografts exhibit elevated levels of cell death, we collected tissue from ungrafted tomato and pepper, self-graft tomato and pepper, and reciprocally heterografted tomato and pepper at 7, 14, and 21 DAG (Fig. S3). To quantify cell death in the junction, we used trypan blue staining to detect regions of deep tissue cell death (Fig. 3, Table S4). We measured a 2.5 mm region of the junction, including any callus present at the interface. When we considered just this sample area, the area of all graft junctions increased at a similar rate, independent of the stem diameter (Fig S5a). To quantify the percent of non-viable tissue (NVT) versus viable tissue, we made a macro in ImageJ to extract tissue that was deeply stained with trypan blue (Fig. 3ak, Fig. S4) and divided this area by the entire area of the junction (Fig S5b). We first analyzed ungrafted tomato (Fig. 3a, g, m) and pepper (Fig. 3b, h, n) stems that were the same age as the grafts we harvested at 7, 14, and 21 DAG. At most, the ungrafted stems from tomato and pepper contained 0.341% and 0.147% NVT respectively. Self-grafted tomato graft junctions consisted of 13.0%

NVT at 7 DAG, which decreased to 3.51% by 21 DAG (Fig. 3u, aa, ag; Wilcoxon Paired Test p = 0.0589). Similarly, self-grafted pepper junctions contained 24.8% NVT at 7 DAG but steadily decreased to only 2.92% by 21 DAG (Fig. 3v, ab, ah; p = 2.78E-02). Unlike the self-grafts, which exhibited decreasing NVT over time, tomato:pepper and pepper:tomato incompatible grafts maintained a consistent percent of NVT over the three week sample period (Fig. 3s-aj). Tomato:pepper junctions contained 20.9%, 20.2%, and 20.8% NVT at 7, 14, and 21 DAG, respectively (Fig. 3w, ac, ai), and reciprocal pepper:tomato junctions exhibited similar levels of NVT: 21.9%, 17.9%, and 17.1% NVT at 7, 14, and 21 DAG, respectively (Fig. 3x, ad, aj). Overall, tomato and pepper exhibited prolonged cell death up to three weeks post-grafting relative to self-grafted controls.

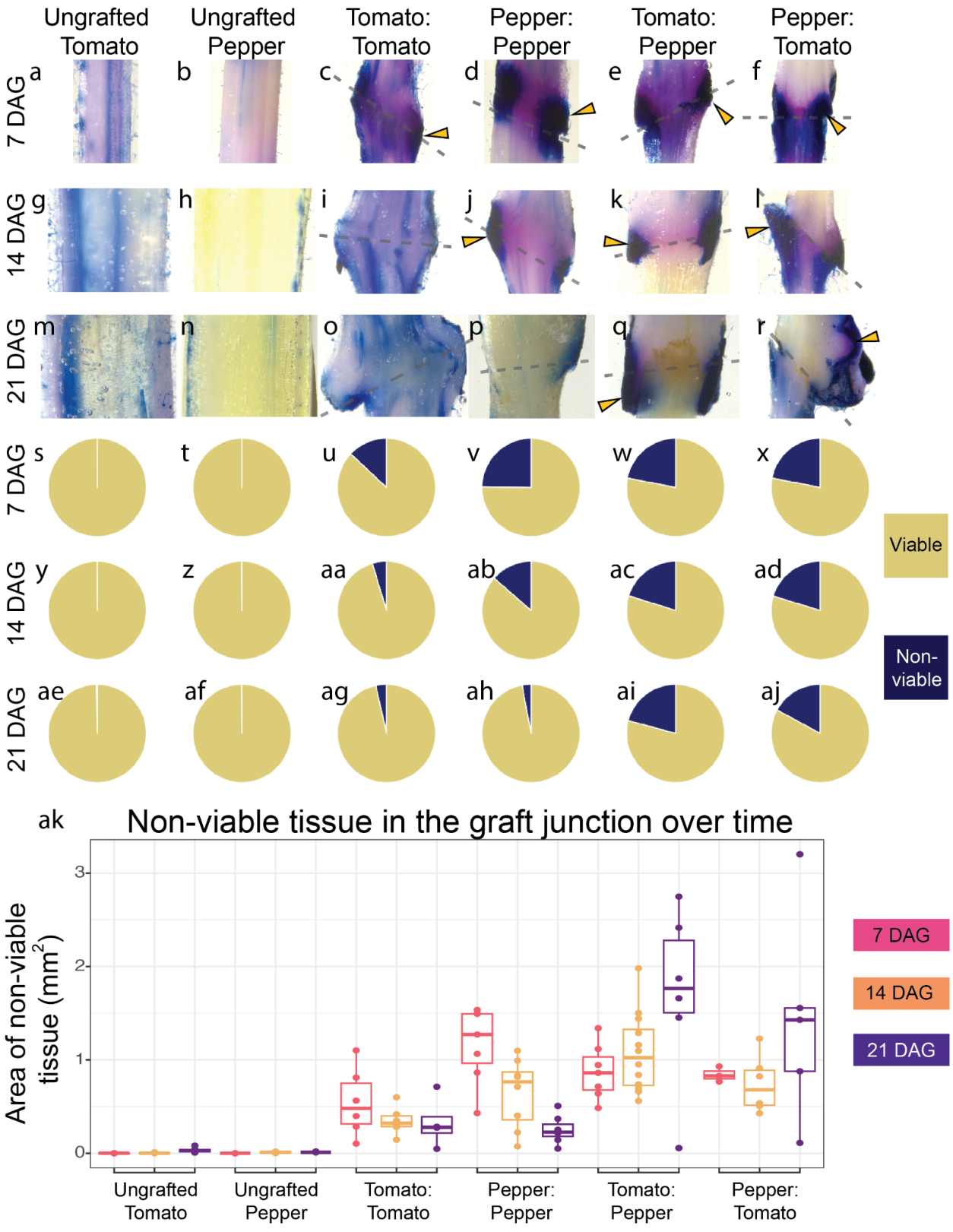

Figure 3: Incompatible grafts contain persistent nonviable tissue over time. (a-r) Representative images of 2.5 mm long graft junctions at 7, 14, and 21 DAG stained with

Trypan Blue. A representative ungrafted tomato stem and the percent of non-viable tissue (NVT) are shown at 7 DAG (a, s), 14 DAG (g, y), and 21 DAG (m, ae). A representative ungrafted pepper stem and the percent of NVT at 7 DAG (b, t), 14 DAG (h, z), and 21 DAG (n, af). A representative self-graft tomato junction and the percent of NVT at 7 DAG (c, u), 14 DAG (i, aa), and 21 DAG (o, ag). A representative self-grafted pepper junction and the percent of NVT at 7 DAG (d, v), 14 DAG (j, ab), and 21 DAG (p, ah). A representative tomato:pepper junction and the percent of NVT at 7 DAG (e, w), 14 DAG (k, ac), and 21 DAG (q, aI). A representative pepper:tomato junction and the percent of NVT at 7 DAG (f, x), 14 DAG (l, ad), and 21 DAG (r, aj). Yellow arrows point to examples of deep tissue death; dashed lines signify the graft site; all junctions are 2.5 mm tall (a-r). (s-aj) The percent of cell death and (ak) the area of cell death in the junction of all graft combinations at 7, 14, and 21 DAG. Pink boxplots are 7 DAG, orange boxplots are 14 DAG, and purple boxplots are 21 DAG. Biological replicates are depicted as jitter (ak) as well as described in detail in Table S4.

Previous work has attributed this incompatible symptom of NVT to the accumulation of trapped cellular debris that creates a necrotic layer in the graft (Tiedemann, 1989). However, the active accumulation of NVT through programmed cell death (PCD) provides an alternative explanation. To test whether NVT accumulation in incompatible grafts was due to PCD, we performed terminal deoxynucleotidyl transferase dUTP nick end labeling (TUNEL) assays on graft junctions from all graft combinations at 7, 14, and 21 DAG (Fig 4, Fig S6-S7). We observed that ungrafted tomato and pepper stems contain cells undergoing PCD at low rates within the stem tissues particularly in xylem and epidermal cells, and indeed PCD could be detected in graft junctions as well (Fig S6-7). Despite detecting PCD in the peripheral areas of the graft junction that overlapped with the region of NVT identified by trypan blue, the high amount of developmental cell death due to vasculogenesis confounded our ability to quantify differences in PCD between compatible (Fig. 4a,b,e,f) and incompatible (Fig. 4c,d,g,h) grafts.

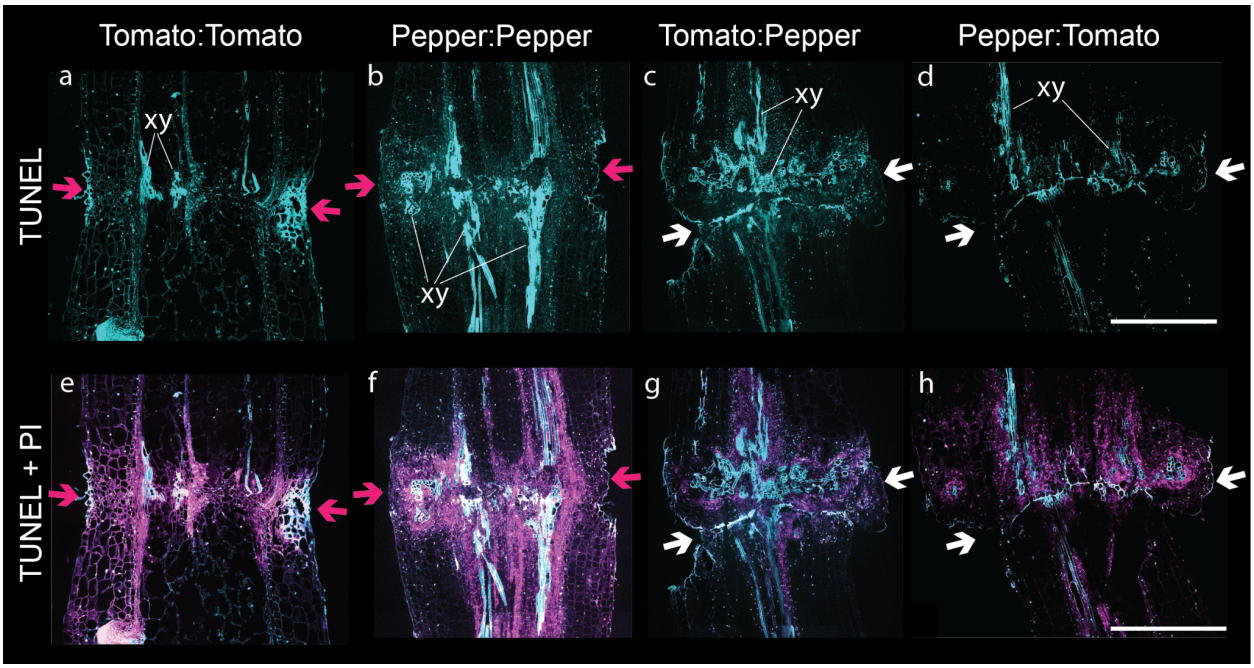

Figure 4: Developmental programmed cell death is present in all graft junctions regardless of compatibility.
A representative graft junction from (a,e) tomato:tomato, (b,f) pepper:pepper, (c,g) tomato:pepper, (d,h) pepper:tomato 14 DAG. (a-d) TUNEL fluorescein-12-dUTP-labeled DNA and autofluorescence are false-colored cyan. (e-h) the TUNEL fluorescence merged with propidium iodide (false-colored magenta) staining nucleic acid and cell walls. Pink arrows indicate a successful graft junction with healed xylem, and white arrows indicate a failed vascular reconnection. Examples of newly developed xylem are labeled (xy). All images are equal and the scale bar is 500 μm.

To understand the cause of the NVT present in the incompatible grafts, we first investigated if DAMPs, which activate PAMP-triggered immunity (PTI) upon cellular rupture during infection and herbivory, also play a role in determining incompatible species combinations (Brutus *et al.*, 2010; Ferrari *et al.*, 2013; Nothnagel *et al.*, 1983). To see if a component of the cell wall could act as an antagonist to inter-species grafting, we designed an *in vitro* assay to test for DAMP-induced changes in callus growth similar to work conducted in quince (Moore, 1986). Tomato and pepper explants were allowed to grow on media containing either tomato or pepper wound exudates for 7 days. If wounding caused the secretion of an inhibitory chemical during callus formation, the hypocotyls growing on cross-species exudates would be stunted. Despite a significant difference in overall growth rates between tomato and pepper explants, the presence of cross-species DAMPs had no effect (Fig. S8, Table S5). Our results

311 indicate that cross-species secreted exudates do not affect callus growth; however, this
312 does not rule out the role of DAMPs in triggering graft-incompatibility during other
313 stages of junction formation.

314 **Tomato and Pepper heterografts express prolonged transcriptional defense**
315 **profiles**

316 To further investigate the underlying cause of NVT in incompatible grafts, we collected
317 and performed RNA-sequencing on ungrafted, self-grafted, and heterografted tissue at
318 7, 14, and 21 DAG (Table S6-7). When compared to ungrafted stems, self-grafted
319 junctions expressed 4.5x, 5x, and 15x less differentially expressed genes compared to
320 heterografts at 7, 14, and 21 DAG, respectively. (Fig. 5, Table S8-9). The reduced
321 number of differentially expressed genes in self-grafts correlates with the healing
322 timeline, where compatible tomato and pepper self-grafts heal within the first week
323 (Thomas *et al.*, 2022).
324

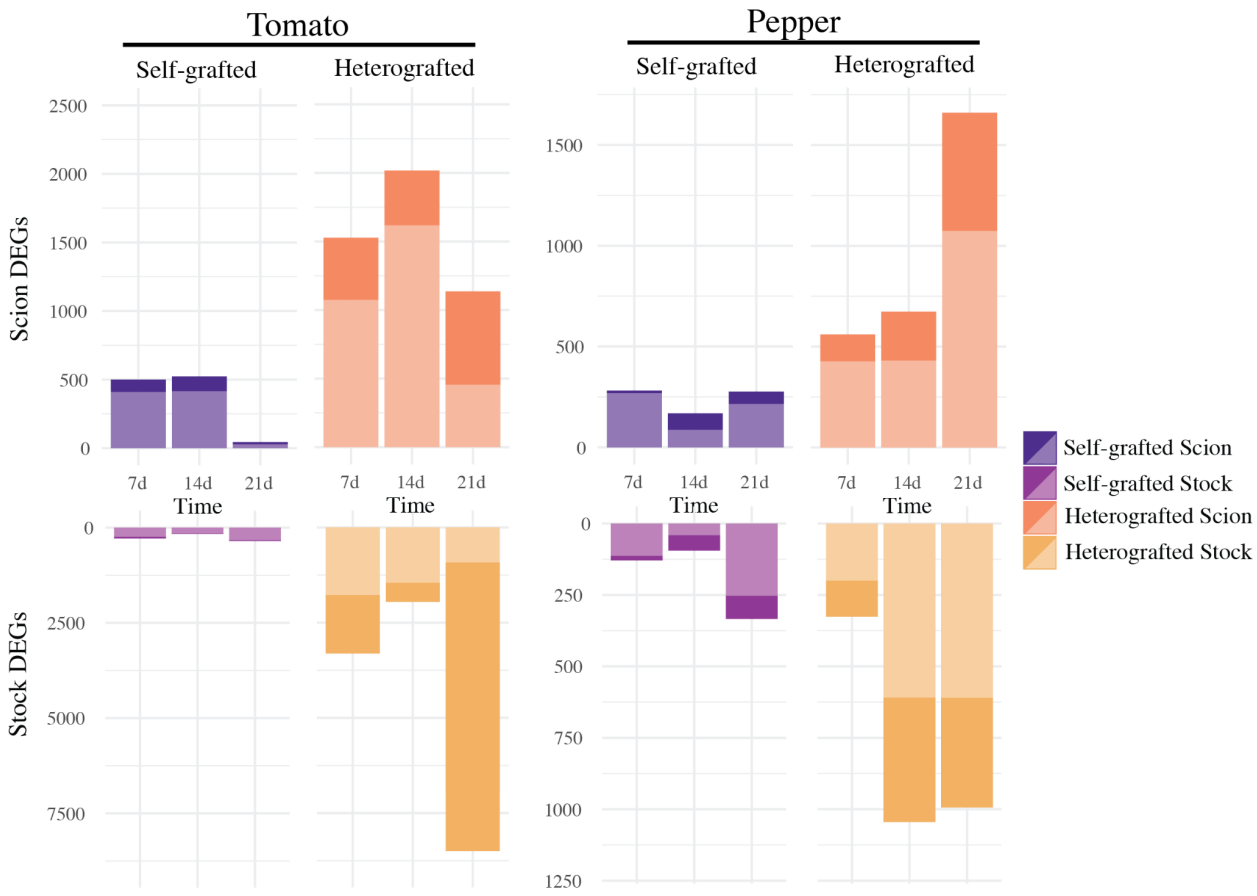

Figure 5: Incompatible heterografts have prolonged differential gene regulation compared to self-grafts. Differentially expressed genes (>1.5 or <-1.5, p-value<0.05) of each grafted tissue (compared to ungrafted) at each time point for tomato and pepper. Upregulated genes are shown in light colors and downregulated genes are shown in dark colors. Self-grafted scions are dark purple, self-grated stocks are light purple, heterografted scions are orange, and heterograft stocks are yellow. Each combination has 3-5 bio-replicates.

To identify genes uniquely upregulated in the incompatible grafts, we used likelihood ratio testing (Table S10). Distinct genes were expressed in the scion and stock, with only a fraction in common at any time point, suggesting that the genetic response in incompatible grafts is spatially and temporally regulated (Fig. S9a-f). For example, at 7 DAG, 1530 and 2380 genes were uniquely upregulated in the scion and stock of incompatible tomato grafts (Fig. S9). Of these 3910 genes, only 576 were shared between scion and stock. The percent of genes upregulated in the scion that were also

upregulated in stock for tomato was only 38%, 2%, and 11% of the total scion DEGs at 7, 14, and 21 DAG respectively. Similarly, genes upregulated in the pepper scion that were also upregulated in the stock made up only 6%, 29%, and 17% of the total scion genes at 7, 14, and 21 DAG. Additionally, scion tissue shared more genes across time than stocks, further supporting that the position in relation to the graft junction, holds a significant role in the genetic process (Fig. S9g-j).

Using significantly upregulated genes from either tomato:pepper or pepper:tomato incompatible graft combinations, we performed GO term enrichment (Figure S10, Table S11). We found that processes associated with defense and stress displayed the highest enrichment in heterografted tomato stocks 14 DAG and pepper stocks 7 DAG (Fig. 6a-b). To further explore how defense processes might be involved in the incompatible response, we targeted NLRs and downstream molecular signaling involved in defense for deeper analysis. Using a collection of 320 previously annotated tomato NLRs (Bashir *et al.*, 2022), we identified 97 defense-related receptors that were significantly upregulated in incompatible grafts (Fig. 6c, Table S12). Of these 97 NLRs, 82 were upregulated in the pepper:tomato 14 DAG sample, indicating this is a critical time point for activating defense-related molecular responses to incompatibility. Similarly, 145 of the 356 annotated pepper NLRs were upregulated during incompatible grafting (Fig. 6d), with a pronounced molecular signature of 101 NLRs upregulated in tomato:pepper grafts 7 DAG (Lee *et al.*, 2021). Notably, stock tissue from both tomato and pepper incompatible grafts exhibit highly upregulated NLR expression within the first two weeks post-grafting (Fig 6a-b). In the absence of an effector protein or pathogen, overexpression of NLRs can trigger autoimmunity that leads to hypersensitive response (HR; Freh *et al.*, 2022). To test whether cell death in incompatible grafts could result from HR, we analyzed the expression of tomato and pepper orthologs EDS1, SAG101, and PAD4, which are known regulators of HR in arabidopsis (Fig. 6e, Table S12; Rietz *et al.*, 2011; Zhu *et al.*, 2011; Gantner *et al.*, 2019). Again, we identified incompatible graft-specific upregulation, especially at 14 DAG, for these HR regulators (Fig. 6e).

Figure 6. Incompatible graft-specific upregulated genes are involved in defense response. (a-b) Uniquely upregulated incompatible graft genes were determined by performing likelihood ratio testing ($p<0.05$) on ungrafted, self-graft scion, and incompatible graft scion as well as ungrafted, self-grafted stock, and incompatible stock tissue. The genes upregulated in only the incompatible graft tissue were used to perform GO enrichment. GO terms enriched in incompatible grafted tomato tissue at 7, 14, and 21 DAG (a). GO terms enriched in incompatible grafted pepper tissue at 7, 14, and 21 DAG (b). (c-d) Log-fold change of NLRs in grafted tissue compared to ungrafted tissue of tomato (c) and pepper (d). (e) The log-fold change of genes involved in hypersensitive response in grafted vs. ungrafted tissue. The log-fold change was scaled by row. The tissue is denoted by the colored columns where self-grafted scions are dark purple, self-grafted stocks are light purple, incompatible grafted scions are orange, and incompatible grafted stocks are yellow. The days after grafting were denoted by colored columns where 7 DAG are white, 14 DAG are grey, and 21 DAG are black. Astrix denotes p-value<0.05 and log-fold change greater than |1.5|.

Next, to explore the role of hormonal regulation in graft compatibility, we identified the closest tomato and pepper putative homologs for annotated Arabidopsis genes involved in salicylic acid (SA), jasmonic acid (JA), and ethylene biosynthesis and response (Fig. S11a-c, Table S12) All three of these hormones are known to play a role in defense processes, with SA serving a critical function in NLR-induced HR (Enyedi *et al.*, 1992; Lorenzo *et al.*, 2003; Koornneef & Pieterse, 2008). In addition, JA and ethylene are associated with graft junction formation (Wang *et al.*, 2020; Thomas *et al.*, 2022). At 7 DAG, SA, JA, and ethylene biosynthesis were upregulated in self and incompatible grafted samples relative to ungrafted controls, indicating that the 7 day response is dominated by general graft healing processes. By 14 and 21 DAG, SA, JA, and ethylene biosynthesis and perception were predominantly upregulated in the incompatible scions compared to self-grafted controls (Fig S11). Congruent with this response, we noticed that the tomato and pepper orthologs for PR1, a defense gene downstream of SA signaling, was upregulated at 21 DAG in incompatible scions. The expression of these genes three-weeks after grafting indicates that the prolonged incompatible graft response is related to defense processes which may be activated or mediated by SA, JA, and ethylene hormonal pathways.

Another hormonal-regulated defense process that was significantly enriched across our incompatible graft time points is the biosynthesis of steroidal glycoalkaloids (SGAs; Fig.

S12, Table S12). SGAs are a class of jasmonate-dependent defensive compounds produced by Solanaceous species (Cárdenas et al. 2016; Milner et al. 2011; Itkin et al. 2013; Panda et al. 2022). Upon further investigation, we were able to find that many genes in SGA biosynthesis (GAME1,4,6,7,11,12,17,18, and MKB1) were significantly upregulated in the incompatible tissue, especially in the scion (Nakayasu *et al.*, 2018). Since this response is shared in tomato and pepper, it is possible that SGA biosynthesis could be triggered by the graft incompatibility immune response (Abdelkareem et al. 2017). Furthermore, SGA content could be a useful metric for gauging graft compatibility in Solanaceae.

We also explored molecular markers for ROS production, which is capable of causing cell death. We examined the expression profiles of known RBOHs (Li *et al.*, 2019; Raziq *et al.*, 2022), and found that of the 8 RBOHs annotated in tomato, only SlRBOH1 and SlRBOHF were both upregulated in incompatible tissue (Fig. S11d, Table S12). Surprisingly, none of the antioxidant enzymes previously shown to be upregulated alongside RBOHs were significantly upregulated in any of our incompatible grafts (Raziq *et al.*, 2022). This data indicates that ROS production is not a dominant by-product of tomato-pepper graft incompatibility at 7 DAG and beyond.

We observed that the stocks of incompatible grafts exhibited high levels of RNA degradation, especially at 21 DAG (Fig. S13). RNA degradation over time in incompatible tissue might be a by-product of genotoxic stress or DNA damage as a part of NLR-activated HR (Rodriguez *et al.*, 2018; Nisa *et al.*, 2019). To see if known genes associated with PCD in Arabidopsis could shed light on the genetic response seen in the incompatible tissue, we identified putative orthologs for programmed cell death indicator genes from Arabidopsis (Olvera-Carrillo *et al.*, 2015). We found that several orthologs for PCD-associated genes were upregulated in incompatible grafts, including HSFB1, ATHB12, and LEA7. Although our TUNEL assays were inconclusive due to the confounding effects of vasculogenesis during graft formation, this data provides molecular support for the role of PCD in promoting persistent cell death in incompatible tomato-pepper graft junctions.

Another interesting group of genes uniquely upregulated in the incompatible grafts were identified plant paralogs to BREAST CANCER SUSCEPTIBILITY GENE 1 (BRCA1, Solyc09g066080, Solyc12g041980) and BRCA1 ASSOCIATED RING DOMAIN PROTEIN 1 (BARD1, Solyc05g016230). In mammals, these genes form a homodimer which is required for homologous recombination, a mode of DNA repair following genotoxic stress. Homologous recombination is a less common method of DNA-repair in eukaryotes, whereas non-homologous end joining is the most prevalent mode. Regardless, the Arabidopsis paralogs for BRCA1/BARD1 are upregulated by genotoxic damage, so it is possible that the NLR-induced immune response in incompatible grafts leads to DNA damage which triggers BRCA1/BARD1. This is especially interesting considering that incompatible tissue showed a genetic overlap with NLR-induced HR, increased defensive processes, an indication of reduced DNA quality over time, and prolonged NVT in the junction. Together this suggests that incompatible grafts might indeed undergo a type of cross-species immune response inducing DNA breakdown and subsequently leading to cell death at the graft junction.

Evolutionary conservation of incompatible tomato and pepper gene families

To determine whether incompatible graft response genes were conserved between tomato and pepper genomes, we generated strict orthogroups between tomato, pepper, and Arabidopsis (Table S14), and then identified significantly upregulated genes (between grafted versus ungrafted controls) with shared ortholog groupings in both tomato and pepper (Tabel S15-16). For instance, out of the 1074 and 428 genes upregulated in the heterografted scions of tomato:pepper and pepper:tomato at 7 DAG, there were 69 orthogroups conserved between the two species. We identified relatively more shared orthogroups in incompatible graft samples versus self-grafted controls, especially with respect to incompatible scion samples (Fig. 7a). Even when considering the magnitude of DEGs between samples, the number of shared orthogroups in incompatible tissue remains proportionately higher than self-grafted tissue. This finding indicates that molecular responses to incompatibility share a high degree of overlap between the tomato and pepper genomes. From this analysis, we identified ERF114

(Solyc03g118190/CA03g31320) as a shared orthogroup that is present in incompatible grafts at 7, 14, and 21 DAG. ERF14 is closely related to RAP2.6L (RELATED to AP2.6L; Fig. 7b), a wound-responsive transcription factor that exhibits overlapping expression with auxin depletion and high levels of JA in stock tissue within the first 24 hours of grafting (Asahina *et al.*, 2011; Matsuoka *et al.*, 2018; Lakehal *et al.*, 2020). Although AtERF114 has not been tested for a direct role in grafting, similar to RAP2.6L, it has been shown to be upregulated under high JA (Lakehal *et al.*, 2020). Incompatible-specific expression of SlERF114 could be explained by its role in ectopic xylem and lateral root formation in arabidopsis (Canher et al. 2022). This hypothesis is supported by the formation of unorganized overproliferated xylem tissue in the incompatible grafts, many of which produce adventitious roots (Fig. 2). These orthologs, much like SGA biosynthesis, serve as candidate markers for detecting incompatibility in Solanaceae.

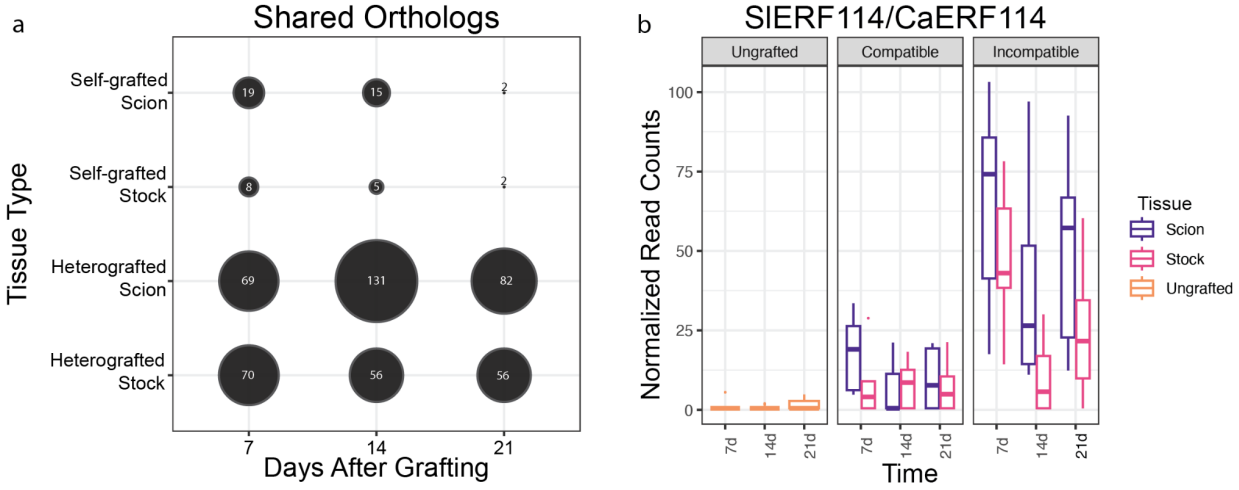

Figure 7. Incompatible grafted plants share many differentially expressed orthologs such as ERF114

(a) Orthologs upregulated at any given tissue/time point in both tomato and pepper. Orthogroups were determined between *Solanum lycopersicum, Capsicum annum,* and *Arabidopsis thaliana* using OrthoFinder. Upregulated genes for all graft combinations were determined in comparison to ungrafted stems. Each gene had a corresponding orthogroup. A shared ortholog was determined if upregulated genes (lfc >1.5, p-value<0.05) from both tomato and pepper at a common tissue/time point were linked to the same orthogroup. (b) Normalized read counts of SlERF114 and CaERF114 were across time. Read counts for tomato and pepper were normalized and faceted by tissue type. Box plots of ungrafted tissue read counts are orange, boxplots of scions tissue read counts are purple, and boxplots of stock tissue read counts are pink.

Incompatible grafting upregulates a set of unique defense processes

Our analyses of incompatible graft responses indicate that both tomato and pepper upregulate strong disease resistance-related molecular responses. To test whether this response is specific to incompatible grafting, or whether these genes share overlapping functions with plant immunity and defense, we compared upregulated incompatible grafting genes with published datasets of three biotic stressors: early plant-parasitism (Jhu *et al.*, 2021), insect herbivory (Ke *et al.*, 2021), and established necrotrophic fungal infections (47 hours post-inoculation; Srivastava *et al.*, 2020). We also used an arbuscular mycorrhizal symbiosis dataset as a control for non-destructive biotic processes (Zeng *et al.*, 2023). Despite these processes occurring in differing tissues and developmental stages, all datasets were moderately correlated with all 7 DAG tomato samples (Spearman Rank average correlation; 0.58; Fig. 8a) and we were able to identify shared transcriptional responses with grafted plants (Fig. 8d-g), as well as between different biotic treatments (Fig. 8b, Table S17). Additionally, all stressors were found to have a significant representation factor (RF) greater than 1 with self and heterografted tissue; meaning that there was a significantly increased overlap of genes upregulated in the stressed tissue and the grafted tissue than expected by chance (Fisher's Exact Test with hypergeometric probability; Table S18). This is in comparison to the Arbuscular mycorrhizal fungi (AMF) dataset, which contained 1385 significantly upregulated genes but lacked enriched overlap with self- or heterografted tissue (Fig. 8d).

Amongst the three biotic stressors analyzed, the necrotrophic fungi, *Botrytis cinerea*, elicited the highest transcriptional responses with 2761 differentially upregulated genes. 223 of these genes were also upregulated in self and incompatible grafts. 541 genes were upregulated in only infected and incompatible grafted tissue (RF: 2.2, Fig. 8e). Shared genes were involved in defense-related processes such as RLKs, MAP kinases, LRR-proteins, and cell death, such as HSR4 (Solyc02g062550; Table S19; Zhang et al. 2014). Plants stressed with herbivory by the tobacco hornworm (*Manduca sexta*)

528 expressed 537 upregulated genes (Fig. 8f). Of these, 44 were shared between
529 herbivory, self-and incompatible grafted plants, 2 were uniquely shared with self-grafted
530 datasets (RF:5.9), and 93 were uniquely shared with incompatible grafts (RF:1.9).
531
532 The parasitic plant, *Cuscuta campestris,* led to 1073 upregulated DEGs, of which 182
533 are shared between parasitized, self-, and incompatible grafted tissue (Fig. 8g). 280
534 genes were both upregulated in only parasitized tissue and incompatible grafts (RF:3.2),
535 while 5 were upregulated in both parasitized and self-grafted, but not incompatible
536 grafts (RF:6.4). The developmental and anatomical processes of parasitic haustorium
537 formation and graft formation share strong parallels; both structures involve tissue
538 reunion and the patterning of newly formed vascular connections. Given these parallels,
539 we hypothesized that parasitism would have the greatest overlap in DEGs with grafted
540 stems, which we found to be especially true for compatible grafts (total gene overlap,
541 RF:5.7). Surprisingly, parasitism also shared the most significant overlap with
542 incompatible grafts out of all 3 biotic stress treatments (total gene overlap, RF: 3.4).
543 Enriched processes in parasitized, self- and heterografted plants include:
544 polysaccharide catabolic processes, response to molecules of fungal origin, defense
545 response to other organisms, and cellular response to oxygen-containing compounds.
546 Genes from these categories include Pathogenesis-related (PR) genes, endochitinases,
547 chitinases, and ethylene biosynthesis components. Genes upregulated in both
548 parasitized tissue and incompatible grafts were enriched for GO terms such as MAPK
549 cascades, regulation of defense responses, regulation of immune response, and
550 defense response to other organisms suggesting that both incompatible grafting and
551 plant parasitism elicit interspecies defense responses.
552
553 While we identified a significant overlap between self-, incompatible grafts, and tissue
554 subjected to the three biotic stressors, we also identified a large set of genes that were
555 uniquely upregulated in grafted samples only (Fig.8c). Self- and incompatible grafts
556 uniquely upregulated 227 genes, and incompatible grafts alone expressed a unique
557 signature of 1019 upregulated genes. These genes were enriched for GO terms
558 including polysaccharide catabolic process and anthocyanin biosynthesis, ABA/salt

559 stress/drought, salicylic acid perception, and response to oxidative stress (Table S20).
560 Within these GO categories, we identified the putative tomato ortholog to AtWRKY70
561 (Solyc03g095770), which functions at the interface of SA and JA signaling (Li *et al.*,
562 2006), in incompatible graft samples at 7 and 14 DAG. Interestingly, the grape ortholog
563 to AtWRKY70 (VIT_08s0058g01390) was previously identified as an upregulated gene
564 in incompatible grape grafts (Assunção *et al.*, 2019), making this gene an extremely
565 interesting candidate for future studies in graft incompatibility.
566

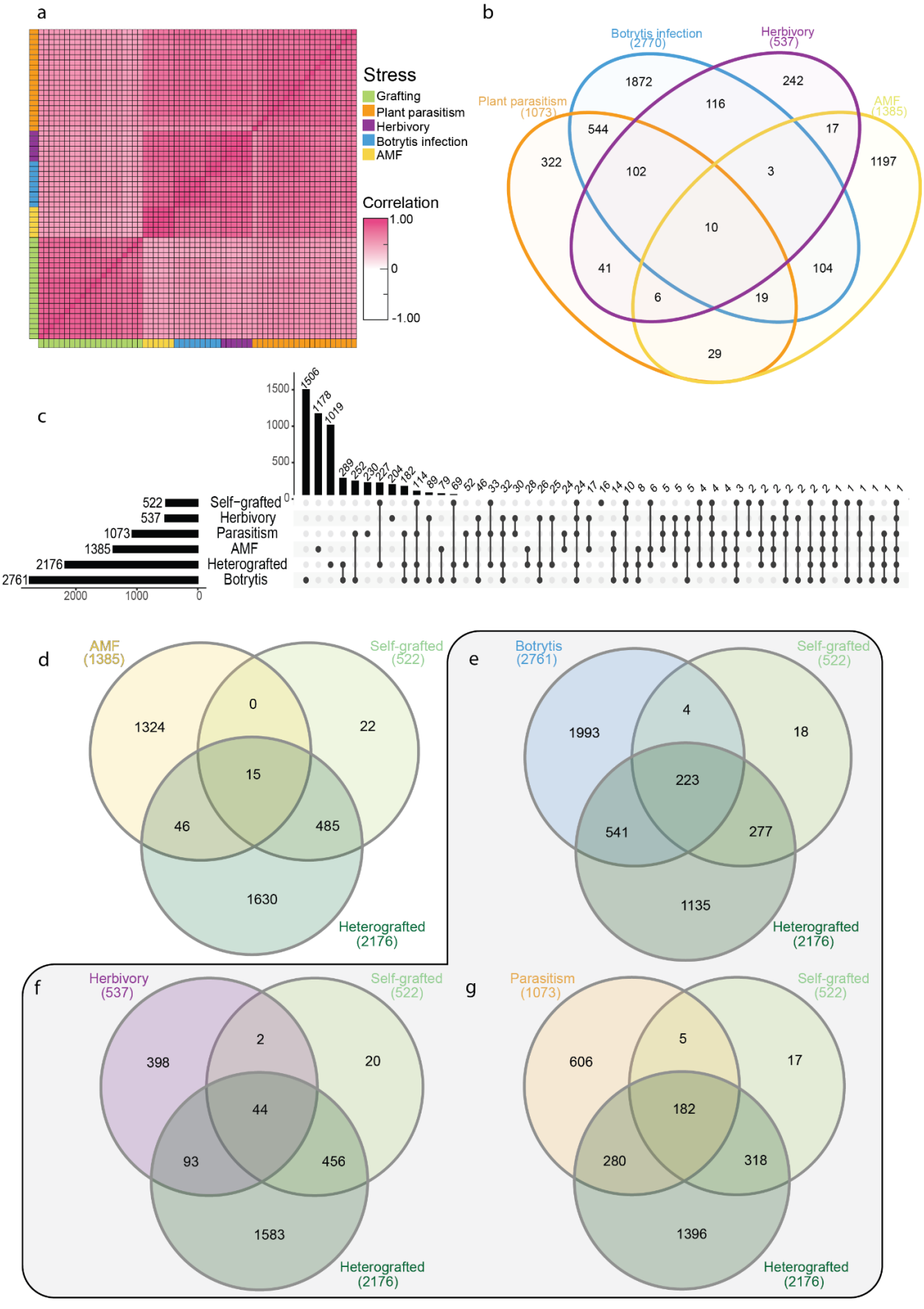

Figure 8: Grafting elicits unique an shared genetic processes with other biological stressors. (a) Spearman Rank Correlation between 7 DAG samples, botrytis infection, herbivory, plant parasitism, and arbuscular mycorrhizal fungi (AMF) colonization. (b) Overlap of upregulated genes from four biological processes investigated. (c) Upset plot showing the overlap between upregulated genes from the biological processes: AMF, plant parasitism, insect herbivory, and fungal infection, scion or stock self-, and scion or stock incompatible graft tissue 7 DAG. (d-g) Overlap of upregulated genes from scion or stock of self- or incompatible-grafted tissue at 7 DAG and all biological processes. (d) The overlap between grafting and AMF, (e) botrytis fungal infection, (f) herbivory, (g) and plant parasitism. The grey outline denotes the biological stressors, whereas AMF was used as a control.

Discussion

In this study, we use an expanded set of germplasm (four pepper varieties from two different *Capsicum* species) to demonstrate that tomato and pepper are broadly incompatible. This assessment is based on the formation of weak graft junctions and failed vascular reconnections between all tomato/pepper combinations (Fig 1). Notably, previous literature cited the Doux des Landes (DDL) pepper variety as graft-compatible with tomato (Deloire & Hébant, 1982). This historic assessment was likely based on high survival rates and the overall healthy appearance of tomato:DDL combinations. However, we demonstrate that along with all other varieties of pepper tested, tomato-DDL grafts fail to form xylem bridges, and as a consequence, develop biophysically unstable junctions that fail the bend test. Based on our findings, we emphasize the importance of verifying anatomical connectivity when diagnosing graft compatibility, and we recommend additional analyses investigating xylem formation and long-term productivity, to unambiguously assess compatible combinations. For all of the heterografts tested, we also were able to show that vascular bridges were not formed and growth was reduced (Fig. 1-2).

In order to analyze cell death in the graft junction, we tracked the percent of non-viable tissue (NVT) in the junction during the first 3 weeks post-grafting (Fig. 3). All grafts exhibited elevated NVT at 7 days after-grafting (DAG), compatible grafts exhibited significantly reduced NVT at 14 and 21 DAG, while incompatible grafts maintained the same percentage of NVT over time. Programmed Cell Death (PCD) is an important genetic mechanism that allows for selective cell death. In addition to its function in

developmental processes (e.g. tracheid and vessel element maturation), PCD plays a central role in specific defense responses, including HR. Due to the high rate of developmental cell death related to vasculogenesis, we were unable to definitively show that PCD caused NVT in incompatible junctions (Fig. 4). To further investigate the cause of sustained NVT in incompatible grafts, we used RNA-seq to analyze the molecular signature of compatible versus incompatible grafts (Fig. 5). In addition to the incompatible grafts displaying a prolonged transcriptional response up to 21 DAG compared to self-grafts, genes upregulated at these later time points were enriched for processes associated with defense responses. Of these upregulated incompatible genes were many NLRs (Fig. 6). NLRs form complexes that monitor both effector presence and effector mediated changes to other proteins; when activated, NLRs trigger ETI and downstream defense responses (Jones *et al.*, 2016). NLRs can also self-activate, triggering an inappropriate immune response (Bomblies *et al.*, 2007; Tran *et al.*, 2017). This phenomenon was originally identified as a type of genetic incompatibility present in F1 offspring of interspecific crosses, leading to the name "hybrid necrosis" (Hollingshead, 1929). Plants executing this immune response display cell death lesions, reduced growth, yellowing, and even complete death (Bomblies & Weigel, 2007). This phenomenon is now attributed to an autoactivated immune response. The neofunctionalization of NLRs in individual species has led to expanded and diverse families, which when crossed can interact deleteriously, activating defense responses in a similar mode to pathogen triggered defense (Tran *et al.*, 2017). The expression of NLRs must remain tightly controlled, since upregulation leads to serious growth penalties (Tian *et al.*, 2003). Furthermore, overexpression of NLRs can be sufficient to activate autoimmunity (Lai & Eulgem, 2018). Like in other instances of NLR autoactivity, where many NLRs are upregulated, we found significant upregulation of the NLRs from both tomato and pepper (Barragan *et al.*, 2021). The *Capsicum* genomes have undergone extensive expansion of the NLR family (Kim *et al.*, 2017). It is possible that the phenotypes we observed in incompatible tomato-pepper grafts are caused by NLR-related genetic incompatibility. This would be the first instance of NLR autoactivation being triggered by physical rather than reproductive genomic combinations. Given that the graft junction is composed of an interspecific fusion of

633 tissues, where the genetic information of tomato and pepper are in intimate proximity, it
634 is logical that grafting could elicit a similar response to hybrid incompatibility.
635 Hypersensitive response requires salicylic acid and a core set of genes PAD4, SAG101,
636 and EDS1 in Arabidopsis. We found that most of the orthologs to these HR regulators,
637 in addition to SA responsive genes, were upregulated in incompatible grafts compared
638 to self-grafted controls. Our molecular evidence points to a model in which tomato-
639 pepper graft incompatibility is caused by an immune response activated by incompatible
640 genetic information, which is perceived by differing NLR alleles present in the tomato
641 and pepper genomes.
642
643 In addition to the shared NLR-upregulation in tomato and pepper heterografts, we also
644 identified a set of shared orthologs that are upregulated in both the tomato and pepper
645 genomes during incompatible grafting. Further analysis of these shared orthologs may
646 help to identify genetic markers for incompatibility in Solanaceae (Fig. 7).
647
648 Next, to explore the genetic fingerprint of graft incompatibility, we compared upregulated
649 genes from compatible grafts, incompatible grafts, and 3 biotic stress datasets
650 (herbivory, fungal infection, and plant parasitism (Fig. 8). We identified an overlap
651 between grafting and these biotic stressors, with a significantly pronounced overlap of
652 upregulated genes between grafting and plant parasitism. Given that the formation of
653 the parasitic haustorium and the graft junction both require inter-specific tissue
654 coordination leading to vascular reconnection, it is logical that the two processes share
655 molecular machinery. The similarity between these two phenomena, both genetically
656 and physiologically, will require future research to fully explore. This analysis also
657 revealed over 1000 uniquely upregulated genes that are expressed in incompatible
658 grafts, including DNA damage repair genes, BRCA1 and BARD1 (Fig 8). Previous work
659 has shown that autoimmune responses caused by NLR overactivation induce DNA
660 damage via EDS1 (Rodriguez *et al.*, 2018). Based on these findings we propose that
661 NLR autoactivation is triggered by genetic incompatibility between the diverged immune
662 systems of tomato and pepper, and this immune response triggers a hypersensitive
663 response producing the prolonged accumulation of non-viable tissue in incompatible

graft junctions that shares similarities with HR-induced lesions. Further supporting our model, our incompatible grafts shared a unique upregulation of DNA damage repair and HR-related genes that are associated with NLR-mediated autoimmunity. From this analysis, we have identified NLR-mediated genetic incompatibility as a likely cause for tomato-pepper graft incompatibility.

Acknowledgments

H.R.T. was supported by a United States Department of Agriculture National Institute of Food and Agriculture (USDA-NIFA) Predoctoral Fellowship (2020-67011-31882); M.H.F., A.G., S.P., and M.N. were supported by the National Science Foundation (NSF) (CAREER IOS-1942437). Imaging data was acquired through the Cornell Institute of Biotechnology's Imaging Facility, with NIH (S10OD018516) funding for the shared Zeiss LSM880 confocal/multiphoton microscope. Access to the Instron Universal testing stand was supported by the Delaware Center for Musculoskeletal Research from the National Institute of Health's National Institute of General Medical Sciences (P20GM139760). Thank you to Noor AlBader for assistance with data transfer.

Competing interests

None to declare.

Author contributions

HRT and MHF designed the study. HRT, AG, AH, SY, LE, MN, and ES carried out the experimentation. HRT analyzed the data. HRT wrote the first draft of the manuscript. All authors contributed critically to the final draft and approval publication.

Data availability

RNA reads collected for this project have been deposited on NCBI GEO (GSE256079). Previously published RNA-seq data used in this research can be accessed on NCBI at PRJNA628162, PRJNA687611, PRJNA756681, PRJNA600385, and PRJNA773605.

References

692 **Abdelkareem A, Thagun C, Nakayasu M, Mizutani M, Hashimoto T, Shoji T**. **2017**.
693 Jasmonate-induced biosynthesis of steroidal glycoalkaloids depends on COI1 proteins in
694 tomato. *Biochemical and biophysical research communications* **489**: 206–210.

695 **Amarante-Mendes GP, Adjemian S, Branco LM, Zanetti LC, Weinlich R, Bortoluci KR**.
696 **2018**. Pattern Recognition Receptors and the Host Cell Death Molecular Machinery. *Frontiers in*
697 *immunology* **9**: 2379.

698 **Andrews PK, Marquez CS**. **2010**. Graft Incompatibility. *Horticultural Reviews*: 183–232.

699 **Argles GK**. **1937**. *A Review of the Literature on Stock-scion Incompatibility in Fruit Trees: With*
700 *Particular Reference to Pome and Stone Fruits*.

701 **Asahina M, Azuma K, Pitaksaringkarn W, Yamazaki T, Mitsuda N, Ohme-Takagi M,**
702 **Yamaguchi S, Kamiya Y, Okada K, Nishimura T, *et al.* 2011**. Spatially selective hormonal
703 control of RAP2.6L and ANAC071 transcription factors involved in tissue reunion in Arabidopsis.
704 *Proceedings of the National Academy of Sciences of the United States of America* **108**: 16128–
705 16132.

706 **Assunção M, Santos C, Brazão J, Eiras-Dias JE, Fevereiro P**. **2019**. Understanding the
707 molecular mechanisms underlying graft success in grapevine. *BMC plant biology* **19**: 396.

708 **Barragan AC, Collenberg M, Wang J, Lee RRQ, Cher WY, Rabanal FA, Ashkenazy H,**
709 **Weigel D, Chae E**. **2021**. A Truncated Singleton NLR Causes Hybrid Necrosis in Arabidopsis
710 thaliana. *Molecular biology and evolution* **38**: 557–574.

711 **Bashir S, Rehman N, Fakhar Zaman F, Naeem MK, Jamal A, Tellier A, Ilyas M, Silva Arias**
712 **GA, Khan MR**. **2022**. Genome-wide characterization of the gene family in tomato () and their
713 relatedness to disease resistance. *Frontiers in genetics* **13**: 931580.

714 **Boller T, He SY**. **2009**. Innate immunity in plants: an arms race between pattern recognition
715 receptors in plants and effectors in microbial pathogens. *Science* **324**: 742–744.

716 **Bomblies K, Lempe J, Epple P, Warthmann N, Lanz C, Dangl JL, Weigel D**. **2007**.
717 Autoimmune response as a mechanism for a Dobzhansky-Muller-type incompatibility syndrome
718 in plants. *PLoS biology* **5**: e236.

719 **Bomblies K, Weigel D**. **2007**. Hybrid necrosis: autoimmunity as a potential gene-flow barrier in
720 plant species. *Nature reviews. Genetics* **8**: 382–393.

721 **Brutus A, Sicilia F, Macone A, Cervone F, De Lorenzo G**. **2010**. A domain swap approach
722 reveals a role of the plant wall-associated kinase 1 (WAK1) as a receptor of oligogalacturonides.
723 *Proceedings of the National Academy of Sciences of the United States of America* **107**: 9452–
724 9457.

725 **Buchfink B, Xie C, Huson DH**. **2014**. Fast and sensitive protein alignment using DIAMOND.
726 *Nature methods* **12**: 59–60.

727 **Burbridge E, Diamond M, Dix PJ, McCabe PF**. **2007**. Use of cell morphology to evaluate the
728 effect of a peroxidase gene on cell death induction thresholds in tobacco. *Plant Science* **172**:
729 853–860.

730 **Cárdenas PD, Sonawane PD, Pollier J, Vanden Bossche R, Dewangan V, Weithorn E, Tal**

L, Meir S, Rogachev I, Malitsky S, *et al.* 2016. GAME9 regulates the biosynthesis of steroidal alkaloids and upstream isoprenoids in the plant mevalonate pathway. *Nature communications* **7**: 10654.

Deloire A, Hébant C. **1982**. Peroxidase Activity and Lignification at the Interface Between Stock and Scion of Compatible and Incompatible Grafts of Capsicum on Lycopersicum. *Annals of Botany* **49**: 887–891.

Eames AJ, Cox LG. **1945**. A REMARKABLE TREE-FALL AND AN UNUSUAL TYPE OF GRAFT-UNION FAILURE. *American Journal of Botany* **32**: 331–335.

Emms DM, Kelly S. **2019**. OrthoFinder: phylogenetic orthology inference for comparative genomics. *Genome biology* **20**: 238.

Ennos AR, Crook MJ, Grimshaw C. **1993**. The Anchorage Mechanics of Maize,Zea mays. *Journal of Experimental Botany* **44**: 147–153.

Enyedi AJ, Yalpani N, Silverman P, Raskin I. **1992**. Localization, conjugation, and function of salicylic acid in tobacco during the hypersensitive reaction to tobacco mosaic virus. *Proceedings of the National Academy of Sciences of the United States of America* **89**: 2480–2484.

Fernández-Bautista, N., Domínguez-Núñez, J. A., Moreno, M. M. C., & Berrocal-Lobo, M. 2016. Plant tissue trypan blue staining during phytopathogen infection. *Bio-protocol*, **6**: e2078-e2078.

Ferrari S, Savatin DV, Sicilia F, Gramegna G, Cervone F, Lorenzo GD. **2013**. Oligogalacturonides: plant damage-associated molecular patterns and regulators of growth and development. *Frontiers in plant science* **4**: 49.

Freh M, Gao J, Petersen M, Panstruga R. **2022**. Plant autoimmunity-fresh insights into an old phenomenon. *Plant physiology* **188**: 1419–1434.

Gantner J, Ordon J, Kretschmer C, Guerois R, Stuttmann J. **2019**. An EDS1-SAG101 Complex Is Essential for TNL-Mediated Immunity in. *The Plant cell* **31**: 2456–2474.

Goodman AM, Ennos AR. **2001**. The Effects of Mechanical Stimulation on the Morphology and Mechanics of Maize Roots Grown in an Aerated Nutrient Solution. *International Journal of Plant Sciences* **162**: 691–696.

Gur, A. 1968. The role of the cyanogensic glycoside of the quince in the incompatibility between pear cultivars and quince rootstocks. *Horticulture Research* **8**: 113-134.

Harrison DJ, Burgess PG. **1962**. Use of rootstock resistance for controlling fusarium wilt of tomatoes. *Plant Pathology* **11**: 23–25.

Hirsch T, Marchetti P, Susin SA, Dallaporta B, Zamzami N, Marzo I, Geuskens M, Kroemer G. **1997**. The apoptosis-necrosis paradox. Apoptogenic proteases activated after mitochondrial permeability transition determine the mode of cell death. *Oncogene* **15**: 1573–1581.

Hollingshead L. **1929**. A Lethal Factor in Crepis Effective Only in an Interspecific Hybrid. *Genetics* **15**: 114-140

Hostetler AN, Erndwein L, Ganji E, Reneau JW, Killian ML, Sparks EE. **2022**. Maize brace

769 root mechanics vary by whorl, genotype, and reproductive stage. *Annals of botany* **126:** 657-
770 668.

771 **Itkin M, Heinig U, Tzfadia O, Bhide AJ, Shinde B, Cardenas PD, Bocobza SE, Unger T,**
772 **Malitsky S, Finkers R, *et al.* 2013**. Biosynthesis of antinutritional alkaloids in solanaceous
773 crops is mediated by clustered genes. *Science* **341**: 175–179.

774 **Ives, L., Brathwaite, R., Barclay, G., Isaac, W. A., Bowen-O'Connor, C., & Bekele, I. 2012.**
775 Graft Compatibility of Scotch Bonnet (*Capsicum chinense Jacq*) with selected salt-tolerant
776 solanaceous. *Journal of Agricultural Science and Technology* **B**: 2(1B).

777 **Janeway, C., Travers, P., Walport, M. and Shlomchik, M., 2001**. *Immunobiology: the immune*
778 *system in health and disease* (Vol. 2, p. 154). New York: Garland Pub..

779 **Jhu M-Y, Farhi M, Wang L, Zumstein K, Sinha NR**. **2021**. Investigating Host and Parasitic
780 Plant Interaction by Tissue-Specific Gene Analyses on Tomato and Interface at Three
781 Haustorial Developmental Stages. *Frontiers in plant science* **12**: 764843.

782 **Jones JDG, Dangl JL**. **2006**. The plant immune system. *Nature* **444**: 323–329.

783 **Jones JDG, Vance RE, Dangl JL**. **2016**. Intracellular innate immune surveillance devices in
784 plants and animals. *Science* **354**.

785 **Kawaguchi M, Taji A, Backhouse D, Oda M**. **2008**. Anatomy and physiology of graft
786 incompatibility in solanaceous plants. *The Journal of Horticultural Science and Biotechnology*
787 **83**: 581–588.

788 **Ke L, Wang Y, Schäfer M, Städler T, Zeng R, Fabian J, Pulido H, De Moraes CM, Song Y,**
789 **Xu S**. **2021**. Transcriptomic Profiling Reveals Shared Signalling Networks Between Flower
790 Development and Herbivory-Induced Responses in Tomato. *Frontiers in plant science* **12**: 722-
791 810.

792 **Kim S, Park J, Yeom S-I, Kim Y-M, Seo E, Kim K-T, Kim M-S, Lee JM, Cheong K, Shin H-S,**
793 ***et al.* 2017**. New reference genome sequences of hot pepper reveal the massive evolution of
794 plant disease-resistance genes by retroduplication. *Genome biology* **18**: 210.

795 **Koornneef A, Pieterse CMJ**. **2008**. Cross talk in defense signaling. *Plant physiology* **146**: 839–
796 844.

797 **Lai Y, Eulgem T**. **2018**. Transcript-level expression control of plant NLR genes. *Molecular plant*
798 *pathology* **19**: 1267–1281.

799 **Lakehal A, Dob A, Rahneshan Z, Novák O, Escamez S, Alallaq S, Strnad M, Tuominen H,**
800 **Bellini C**. **2020**. ETHYLENE RESPONSE FACTOR 115 integrates jasmonate and cytokinin
801 signaling machineries to repress adventitious rooting in Arabidopsis. *The New phytologist* **228**:
802 1611–1626.

803 **Lee H, Mang H, Choi E, Seo Y, Kim M, Oh S, Kim S, Choi D**. **2021**. Genome-wide functional
804 analysis of hot pepper immune receptors reveals an autonomous NLR clade in seed plants.
805 *New Phytologist* **229**: 532–547.

806 **Li J, Brader G, Kariola T, Palva ET**. **2006**. WRKY70 modulates the selection of signaling
807 pathways in plant defense. *The Plant journal: for cell and molecular biology* **46**: 477–491.

Li X, Li Y, Ahammed GJ, Zhang X-N, Ying L, Zhang L, Yan P, Zhang L-P, Li Q-Y, Han W-Y. **2019**. RBOH1-dependent apoplastic H2O2 mediates epigallocatechin-3-gallate-induced abiotic stress tolerance in Solanum lycopersicum L. *Environmental and experimental botany* **161**: 357–366.

Lockshin RA, Zakeri Z. **2004**. Apoptosis, autophagy, and more. *The International Journal of Biochemistry & Cell Biology* **36**: 2405–2419.

Lorenzo O, Piqueras R, Sánchez-Serrano JJ, Solano R. **2003**. ETHYLENE RESPONSE FACTOR1 integrates signals from ethylene and jasmonate pathways in plant defense. *The Plant cell* **15**: 165–178.

Love MI, Huber W, Anders S. **2014**. Moderated estimation of fold change and dispersion for RNA-seq data with DESeq2. *Genome biology* **15**: 550.

Matsuoka K, Yanagi R, Yumoto E, Yokota T, Yamane H, Satoh S, Asahina M. **2018**. RAP2.6L and jasmonic acid-responsive genes are expressed upon Arabidopsis hypocotyl grafting but are not needed for cell proliferation related to healing. *Plant molecular biology* **96**: 531–542.

Melnyk CW, Schuster C, Leyser O, Meyerowitz EM. **2015**. A Developmental Framework for Graft Formation and Vascular Reconnection in Arabidopsis thaliana. *Current biology: CB* **25**: 1306–1318.

Mendel K. **1936**. The Anatomy and Histology of the Bud-union in Citrus. *Palestine Journal of Botanical and Horticultural Science* **1**: 13-46

Milner SE, Brunton NP, Jones PW, O'Brien NM, Collins SG, Maguire AR. **2011**. Bioactivities of glycoalkaloids and their aglycones from Solanum species. *Journal of agricultural and food chemistry* **59**: 3454–3484.

Moore R. **1981**. Graft compatibility and incompatibility in higher plants. *Developmental and comparative immunology* **5**: 377–389.

Moore R. **1983**. Studies of vegetative compatibility-incompatibility in higher plants. Iv. The development of tensile strength in a compatible and an incompatible graft. *American Journal of Botany* **70**: 226–231.

Moore R. **1984**. A model for graft compatibility-incompatibility in higher plants. *American Journal of Botany* **71**: 752–758.

Moore R. **1986**. Graft incompatibility between pear and quince: the influence of metabolites of *Cydonia oblonga* on suspension cultures of *Pyrus communis*. *American journal of botany* **73**: 1–4.

Moore R, Walker DB. **1981**. Studies of vegetative compatibility-incompatibility in higher plants. Ii. A structural study of an incompatible heterograft between *Sedum telephoides* (crassulaceae) and *Solanum pennellii* (solanaceae). *American Journal of Botany* **68**: 831–842.

Mosse B, Herrero J. **1951**. Studies on Incompatibility Between Some Pear and Quince Grafts. *Journal of Horticultural Science* **26**: 238–245.

Mudge K, Janick J, Scofield S, Goldschmidt EE. **2009**. A History of Grafting. *Horticultural*

Reviews: 437–493.

Nakayasu M, Shioya N, Shikata M, Thagun C, Abdelkareem A, Okabe Y, Ariizumi T, Arimura G-I, Mizutani M, Ezura H, *et al.* 2018. JRE4 is a master transcriptional regulator of defense-related steroidal glycoalkaloids in tomato. *The Plant journal: for cell and molecular biology* **94**: 975–990.

Nisa M-U, Huang Y, Benhamed M, Raynaud C. **2019**. The Plant DNA Damage Response: Signaling Pathways Leading to Growth Inhibition and Putative Role in Response to Stress Conditions. *Frontiers in plant science* **10**: 653.

Nothnagel EA, McNeil M, Albersheim P, Dell A. **1983**. Host-Pathogen Interactions : XXII. A Galacturonic Acid Oligosaccharide from Plant Cell Walls Elicits Phytoalexins. *Plant physiology* **71**: 916–926.

Olvera-Carrillo Y, Van Bel M, Van Hautegem T, Fendrych M, Huysmans M, Simaskova M, van Durme M, Buscaill P, Rivas S, Coll NS, *et al.* 2015. A Conserved Core of Programmed Cell Death Indicator Genes Discriminates Developmentally and Environmentally Induced Programmed Cell Death in Plants. *Plant physiology* **169**: 2684–2699.

Panda S, Jozwiak A, Sonawane PD, Szymanski J, Kazachkova Y, Vainer A, Vasuki Kilambi H, Almekias-Siegl E, Dikaya V, Bocobza S, *et al.* 2022. Steroidal alkaloids defence metabolism and plant growth are modulated by the joint action of gibberellin and jasmonate signalling. *The New phytologist* **233**: 1220–1237.

R Core Team. 2021. R: A language and environment for statistical computing. R Foundation for Statistical Computing.

Raziq A, Wang Y, Mohi Ud Din A, Sun J, Shu S, Guo S. **2022**. A Comprehensive Evaluation of Salt Tolerance in Tomato (Var. Ailsa Craig): Responses of Physiological and Transcriptional Changes in RBOH's and ABA Biosynthesis and Signalling Genes. *International journal of molecular sciences* **23**.

Rietz S, Stamm A, Malonek S, Wagner S, Becker D, Medina-Escobar N, Corina Vlot A, Feys BJ, Niefind K, Parker JE. **2011**. Different roles of Enhanced Disease Susceptibility1 (EDS1) bound to and dissociated from Phytoalexin Deficient4 (PAD4) in Arabidopsis immunity. *The New phytologist* **191**: 107–119.

Rodriguez E, Chevalier J, El Ghoul H, Voldum-Clausen K, Mundy J, Petersen M. **2018**. DNA damage as a consequence of NLR activation. *PLoS genetics* **14**: e1007235.

Srivastava DA, Arya GC, Pandaranayaka EP, Manasherova E, Prusky DB, Elad Y, Frenkel O, Harel A. **2020**. Transcriptome Profiling Data of Infection on Whole Plant. *Molecular plant-microbe interactions: MPMI* **33**: 1103–1107.

Steinbrenner AD, Muñoz-Amatriaín M, Chaparro AF, Aguilar-Venegas JM, Lo S, Okuda S, Glauser G, Dongiovanni J, Shi D, Hall M, *et al.* 2020. A receptor-like protein mediates plant immune responses to herbivore-associated molecular patterns. *Proceedings of the National Academy of Sciences of the United States of America* **117**: 31510–31518.

Stergiopoulos I, de Wit PJGM. **2009**. Fungal effector proteins. *Annual review of phytopathology* **47**: 233–263.

887 **Thomas HR, Gevorgyan A, Frank MH**. **2023**. Anatomical and biophysical basis for graft
888 incompatibility within the Solanaceae. *Journal of experimental botany* **74**: 4461–4470.

889 **Thomas H, Van den Broeck L, Spurney R, Sozzani R, Frank M**. **2022**. Gene regulatory
890 networks for compatible versus incompatible grafts identify a role for SlWOX4 during junction
891 formation. *The Plant cell* **34**: 535–556.

892 **Tian D, Traw MB, Chen JQ, Kreitman M, Bergelson J**. **2003**. Fitness costs of R-gene-
893 mediated resistance in Arabidopsis thaliana. *Nature* **423**: 74–77.

894 **Tiedemann R**. **1989**. Graft Union Development and Symplastic Phloem Contact in the
895 Heterograft Cucumis sativus on Cucurbita ficifolia. *Journal of Plant Physiology* **134**: 427–440.

896 **Tran DTN, Chung E-H, Habring-Müller A, Demar M, Schwab R, Dangl JL, Weigel D, Chae**
897 **E**. **2017**. Activation of a Plant NLR Complex through Heteromeric Association with an
898 Autoimmune Risk Variant of Another NLR. *Current biology: CB* **27**: 1148–1160.

899 **Waldman, A. D., Fritz, J. M., & Lenardo, M. J. 2020.** A guide to cancer immunotherapy: from T
900 cell basic science to clinical practice. Nature Reviews Immunology, **20**: 651-668

901 **Walker-Simmons M , Hollander-Czytko H, Andersen JK, Ryan CA. 1984.** Wound signals in
902 plants: a systemic plant wound signal alters plasma membrane integrity. Proceedings of the
903 National Academy of Sciences: **81**.12: 3737-3741.

904 **Wang J, Li D, Chen N, Chen J, Mu C, Yin K, He Y, Liu H**. **2020**. Plant grafting relieves
905 asymmetry of jasmonic acid response induced by wounding between scion and rootstock in
906 tomato hypocotyl. *PloS one* **15**: e0241317.

907 **Warschefsky EJ, Klein LL, Frank MH, Chitwood DH, Londo JP, von Wettberg EJB, Miller**
908 **AJ**. **2016**. Rootstocks: Diversity, Domestication, and Impacts on Shoot Phenotypes. *Trends in*
909 *plant science* **21**: 418–437.

910 **Williams B, Ahsan MU, Frank MH**. **2021**. Getting to the root of grafting-induced traits. *Current*
911 *opinion in plant biology* **59**: 101988.

912 **Wu L, Chen H, Curtis C, Fu ZQ**. **2014**. Go in for the kill: How plants deploy effector-triggered
913 immunity to combat pathogens. [Corrected]. *Virulence* **5**: 710–721.

914 **Zeist AR, Giacobbo CL, da Silva Neto GF, Zeist RA, da R Dorneles K, de Resende JTV**.
915 **2018**. Compatibility of tomato cultivar Santa Cruz Kada grafted on different Solanaceae species
916 and control of bacterial wilt. *Horticultura Brasileira* **36**: 377–381.

917 **Zeng Z, Liu Y, Feng X-Y, Li S-X, Jiang X-M, Chen J-Q, Shao Z-Q**. **2023**. The RNAome
918 landscape of tomato during arbuscular mycorrhizal symbiosis reveals an evolving RNA layer
919 symbiotic regulatory network. *Plant communications* **4**: 100429.

920 **Zhu S, Jeong R-D, Venugopal SC, Lapchyk L, Navarre D, Kachroo A, Kachroo P**. **2011**.
921 SAG101 forms a ternary complex with EDS1 and PAD4 and is required for resistance signaling
922 against turnip crinkle virus. *PLoS pathogens* **7**: e1002318.

923

924

Figure Legends

Figure 1: Heterografted tomato and pepper combinations exhibit moderate survival, unstable stem integrity, and reduced growth. The relationship between percent survival (y-axis) and percent break (x-axis) is shown for all graft combinations (a). Black dots denote self-grafts, grey dots denote heterografts. Self-grafted tomato is outlined in orange. Self-grafted pepper is outlined in green. Heterografts where the scion is tomato are outlined in purple. Heterografts where the stock is tomato are outlined in blue. The identity of each data point is labeled 1-13. Percent survival n=30; For bend test sample size see Table S1. The change in stem diameter 2cm above the graft junction between 30 and 0 DAG (scion) (b). The change in stem diameter 2 cm below the graft junction between 30 and 0 DAG (stock) (c). California Wonder abbreviated to Cali Wonder, Doux des Landes abbreviated to DDL. Biological replicates are depicted as jitter and described in Table S2. Kruskal–Wallis one-way analysis of variance was used to detect significant differences between self-and heterografted combinations. p-value <0.05.

Figure 2: Heterografted pepper fails to form vascular connections and shows a significant decrease in size 30 DAG. (a, c, e, g, i, k, m, o, q, s, w, u, w, y) Representative photographs and (b, d, f, h, j, l, n, p, r, t, v, x, z) confocal micrographs for self-grafted tomato (a-b), self-grafted habanero (c-d), tomato:Habanero (e-f), Habanero:tomato (g-h), self-grafted Doux des Landes (DDL) (i-j), tomato:DDL (k-l), DDL:tomato (m-n). self-grafted Cayenne (o-p), tomato:Cayenne (q-r), Cayenne:tomato (s-t), self-grafted California Wonder (CW) (u-v), tomato:CW (w-x), CW:tomato (y-z). Graft junctions were stained with propidium iodide and imaged on a confocal microscope. Pink arrows indicate a successful graft junction with a healed xylem, white arrows indicate a failed vascular reconnection and white Asterix highlight adventitious roots. All plant images have scale bars are 5 cm, and all micrograph scale bars are 1000 µm.

Figure 3: Incompatible grafts contain persistent nonviable tissue over time. (a-r) Representative images of 2.5 mm long graft junctions at 7, 14, and 21 DAG stained with Trypan Blue. A representative ungrafted tomato stem and the percent of non-viable tissue (NVT) are shown at 7 DAG (a, s), 14 DAG (g, y), and 21 DAG (m, ae). A representative ungrafted pepper stem and the percent of NVT at 7 DAG (b, t), 14 DAG (h, z), and 21 DAG (n, af). A representative self-graft tomato junction and the percent of NVT at 7 DAG (c, u), 14 DAG (i, aa), and 21 DAG (o, ag). A representative self-grafted pepper junction and the percent of NVT at 7 DAG (d, v), 14 DAG (j, ab), and 21 DAG (p, ah). A representative tomato:pepper junction and the percent of NVT at 7 DAG (e, w), 14 DAG (k, ac), and 21 DAG (q, al). A representative pepper:tomato junction and the percent of NVT at 7 DAG (f, x), 14 DAG (l, ad), and 21 DAG (r, aj). Yellow arrows point to examples of deep tissue death; dashed lines signify the graft site; all junctions are 2.5 mm tall (a-r). (s-aj) The percent of cell death and (ak) the area of cell death in the junction of all graft combinations at 7, 14, and 21 DAG. Pink boxplots are 7 DAG,

orange boxplots are 14 DAG, and purple boxplots are 21 DAG. Biological replicates are depicted as jitter (ak) as well as described in detail in Table S4.

Figure 4: Developmental programmed cell death is present in all graft junctions regardless of compatibility. A representative graft junction from (a,e) tomato:tomato, (b,f) pepper:pepper, (c,g) tomato:pepper, (d,h) pepper:tomato 14 DAG. (a-d) TUNEL fluorescein-12-dUTP-labeled DNA and autofluorescence are false-colored cyan. (e-h) the TUNEL fluorescence merged with propidium iodide (false-colored magenta) staining nucleic acid and cell walls. Pink arrows indicate a successful graft junction with healed xylem, and white arrows indicate a failed vascular reconnection. Examples of newly developed xylem are labeled (xy). All images are equal and the scale bar is 500 μm.

Figure 5: Incompatible heterografts have prolonged differential gene regulation compared to self-grafts. Differentially expressed genes (>1.5 or <-1.5, p-value<0.05) of each grafted tissue (compared to ungrafted) at each time point for tomato and pepper. Upregulated genes are shown in light colors and downregulated genes are shown in dark colors. Self-grafted scions are dark purple, self-grated stocks are light purple, heterografted scions are orange, and heterograft stocks are yellow. Each combination has 3-5 bio-replicates.

Figure 6. Heterograft-specific upregulated genes are involved in defense response. (a-b) Uniquely upregulated heterografted genes were determined by performing likelihood ratio testing (p<0.05) on ungrafted, self-graft scion, and heterografted scion as well as ungrafted, self-grafted stock, and heterografted stock tissue. The genes upregulated in only the heterograft tissue were used to perform GO enrichment. GO terms enriched in heterografted tomato tissue at 7, 14, and 21 DAG (a). GO terms enriched in heterografted pepper tissue at 7, 14, and 21 DAG (b). (c-d) Log-fold change of NLRs in grafted tissue compared to ungrafted tissue of tomato (c) and pepper (d). (e) The log-fold change of genes involved in hypersensitive response in grafted vs. ungrafted tissue. The log-fold change was scaled by row. The tissue is denoted by the colored columns where self-grafted scions are dark purple, self-grafted stocks are light purple, heterografted scions are orange, and heterografted stocks are yellow. The days after grafting were denoted by colored columns where 7 DAG are white, 14 DAG are grey, and 21 DAG are black. Asterisks denotes p-value<0.05 and log-fold change greater than |1.5|.

Figure 7. Heterografted plants share many differentially expressed putative orthologs such as ERF114

(a) Putative orthologs upregulated at any given tissue/time point in both tomato and pepper. Orthogroups were determined between *Solanum lycopersicum, Capsicum annum,* and *Arabidopsis thaliana* using OrthoFinder, where each gene corresponded to an orthogroup. Upregulated genes for all graft combinations were determined in comparison to ungrafted stems. A shared ortholog was determined if upregulated genes (lfc >1.5, p-value<0.05) from both tomato and pepper at a common tissue/time point were linked to the same orthogroup. (b) Normalized read counts of SlERF114 and CaERF114 across time. Read counts for tomato and pepper were normalized,

combined, and faceted by tissue type. Boxplot color denotes tissue origin; Ungrafted tissue is orange, scion tissue is purple, and stock tissue is pink.

Figure 8: Grafting elicits unique and shared genetic processes with other biological stressors. (a) Spearman Rank Correlation between 7 DAG samples, botrytis infection, herbivory, plant parasitism, and arbuscular mycorrhizal fungi (AMF) colonization. (b) Overlap of upregulated genes from four biological processes investigated. (c) Upset plot showing the overlap between upregulated genes from the biological processes: AMF, plant parasitism, insect herbivory, and fungal infection, scion or stock self-, and scion or stock heterografted tissue 7 DAG. (d-g) Overlap of upregulated genes from scion or stock of self- or hetero-grafted tissue at 7 DAG and all biological processes. (d) The overlap between grafting and AMF, (e) botrytis fungal infection, (f) herbivory, (g) and plant parasitism. The grey outline denotes the biological stressors, whereas AMF was used as a control.

Supporting Information

Fig. S1 Tomato and pepper heterografts have reduced survival and weak graft junctions.
Fig. S2 Incompatible grafts have reduced secondary growth 30 DAG.
Fig. S3 Tomato and pepper grafts were collected at 7, 14, and 21 DAG for TUNEL assays, trypan blue, and RNA-seq
Fig. S4 Non-viable tissue was quantified in ImageJ
Fig. S5 Heterografted tomato and pepper have consistent growth and persistent non-viable tissue
Fig. S6 All grafted plants have elevated programmed cell death in the graft junction
Fig. S7 All grafted plants have elevated programmed cell death in the graft junction (merged)
Fig. S8 Cross-species exudates do not affect callus growth of tomato or pepper
Fig. S9 Genetic overlap between tomato and pepper grafts shows scion-stock specificity.
Fig. S10 Scion and stock tissue have distinct upregulated genes at any given time point
Fig. S11 Hormonal regulation but not ROS production is upregulated in incompatible grafts
Fig. S12 DNA quality decreases over time in incompatible stocks
Fig. S13 The steroidal glycoalkaloid biosynthesis pathway is significantly upregulated in heterografted grafted scions.
Fig.S14 Biological stressors upregulate distinct and shared genetic responses

Method S1 Plant material and growth conditions
Method S2 Grafting
Method S3 Pepper Compatibility Grafts
Method S4 Propidium Iodide Staining
Method S5 Bend Test
Method S6 Instron three-point bend test